Supplementary Information

Polymer-Confined Growth of Perovskite–PAN Composite Micro-ring Arrays for Uniform and Stable Lasing

Xuanyue Li,[†] *Haihua Zhang,*[*,†] *Dexiang Zhu,*[†] *Hongbing Fu*[*,†,‡]

† Institute of Molecular Plus (IMP), Collaborative Innovation Center of Chemical Science and Engineering (Tianjin), National Industry-Education Platform for Energy Storage (Tianjin), Tianjin University, Tianjin 300072, P. R. China.

‡ Beijing Key Laboratory for Optical Materials and Photonic Devices, Department of Chemistry, Capital Normal University, Beijing 100048, P. R. China.

* Email: zhanghaihua@tju.edu.cn; hbfu@cnu.edu.cn

KEYWORDS: Perovskite, Polyacrylonitrile, Micro-ring array, In situ growth, Lasing

Table of Contents

1. **Experimental Section**
2. **Fig. S1** PDMS template used for microring fabrication: (a) optical image; (b) enlarged view of the ring-patterned grooves.
3. **Fig. S2** μ-PL spectra (a) and SEM images (b) of $MAPbBr_3$ micro-ring arrays.
4. **Fig. S3** XPS spectra (Pb 4f and N1s) of the $MAPbBr_3$ films and $MAPbBr_3$@PAN composite films.
5. **Fig. S4** Schematic illustration of the home-built micro-photoluminescence (μ-PL) setup used for lasing measurements.
6. **Fig. S5** Pump-fluence-dependent PL characterization of $MAPbBr_3$@PAN composite films with different PAN addition amounts.
7. **Fig. S6** Pump-fluence-dependent PL characterization of $MAPbBr_3$@PAN micro-rings for lasing threshold statistics in Fig. 2c.
8. **Fig. S7** Laser spectral stability of $MAPbBr_3$@PAN micro-ring under high humidity conditions (20 ℃, 60% humidity).
9. **Fig. S8** The lasing spectra of $MAPbBr_3$@PAN micro-ring uder different laser shots.
10. **Fig. S9** (a) μ-PL spectra of $MAPbX_3$@PAN micro-rings (b) Integrated μ-PL intensities versus pump density.
11. **Tab. S1** Comparative summary of key parameters in micro/nanolaser arrays.

Experimental Section

1.1 Materials.

All perovskite starting materials (MABr, $PbBr_2$, $PbCl_2$, PbI_2) were purchased from Xi'an Polymer Light Technology Corp. Polyacrylonitrile (PAN, Mw=100000) was purchased from Marklin. The N,N-Dimethylformamide (DMF, HPLC grade) was purchased from Beijing Chemical Agent Ltd., China.

1.2 Preparation of $MAPbBr_3$@PAN solution

The $MAPbBr_3$ perovskite solution was prepared by dissolving MABr and $PbBr_2$ in DMF, with the Pb^{2+} concentration fixed at 0.1 mol/L. Subsequently, PAN was dissolved into this solution and stirred at 60 °C for 2 hours to obtain the $MAPbBr_3$@PAN solution.

1.3 Preparation of polydimethylsiloxane (PDMS) template.

The PDMS template was fabricated by replica molding against a silicon master mold featuring micro-ring convex structures prepared by photolithography. After curing, the PDMS template was peeled off from the silicon mold and cut into 1×1 cm^2 pieces prior to use. The diameter of the PDMS template (D = 20 μm) is determined by the diameter of the convex silicon micro-rings.

1.4 Morphology and Structure Measurements.

The morphologies using field emission scanning electron microscopy (FESEM, Thermo Fisher Scientific) at acceleration voltages of 10 kV. Microrings fabricated via the PDMS-assisted growth method require no sectioning treatment. These microrings are distributed independently and uniformly on the glass substrate. These microrings are distributed independently and uniformly on the glass substrate. A large number of microrings on the substrate can be transferred onto a copper grid using PDMS, and the transferred sample can be directly observed. Transmission

electron microscopy measurements were performed on a Thermo Scientific Talos F200X instrument at an accelerating voltage of 200 kV.

1.5 Laser Measurements.

Laser measurements were conducted using a homebuilt inverted fluorescence microscope equipped with a 40× objective (NA = 0.9). The output from an optical parametric amplifier (Orp heus, Light Conversion; 400 nm, 1 kHz) was focused to a spot with a diameter of 200 μm. Photoluminescence (PL) spectra were acquired in a reflection configuration, with a movable aperture placed in the optical path at the front focal plane. The signal was collected and detected by a liquid-nitrogen-cooled CCD camera.

Additional Information

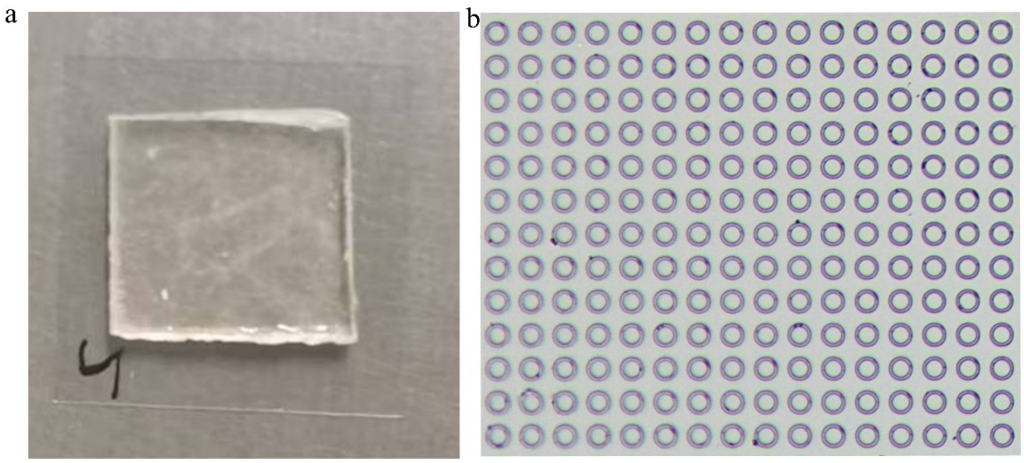

Fig. S1 PDMS template used for microring fabrication: (a) optical image; (b) enlarged view of the ring-patterned grooves.

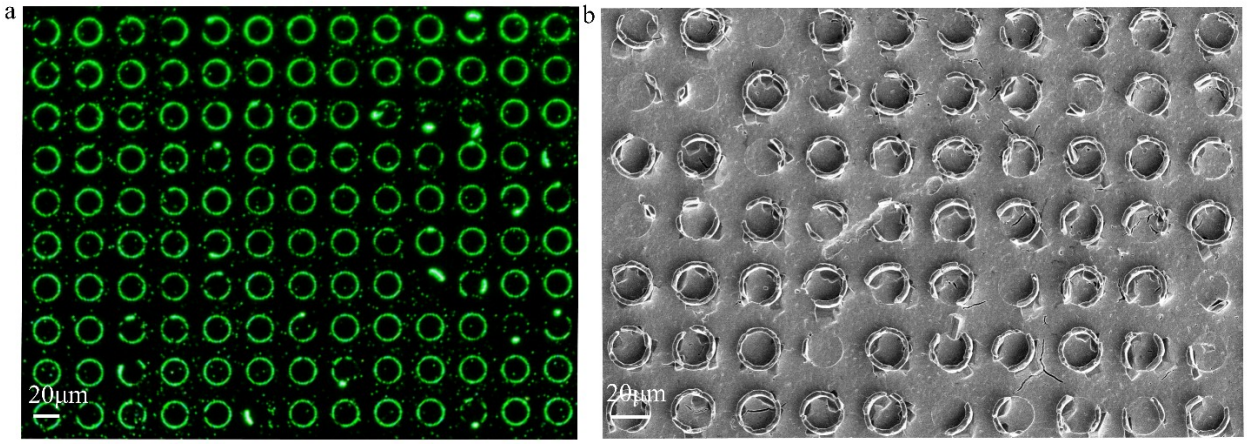

Fig. S2 μ-PL spectra (a) and SEM images (b) of $MAPbBr_3$ micro-ring arrays.

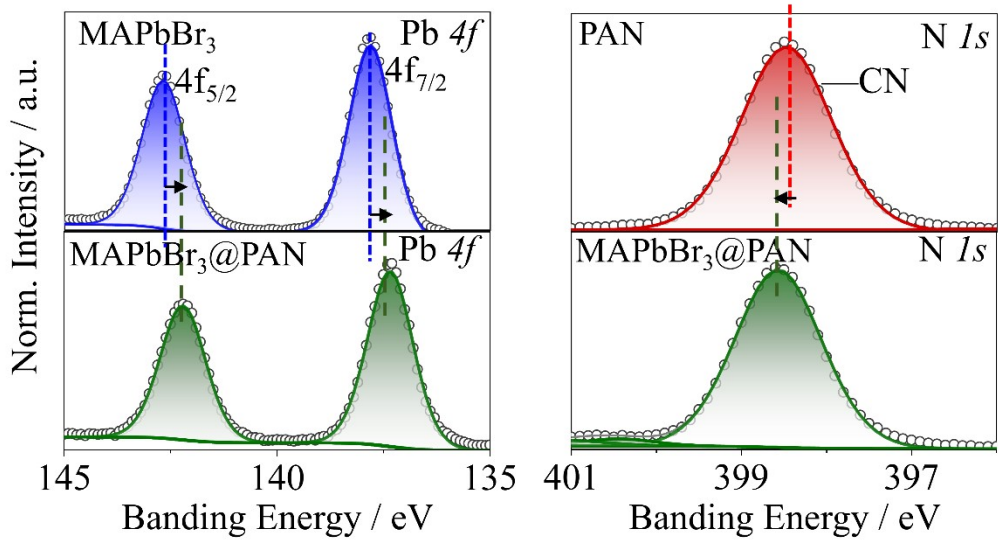

Fig. S3 XPS spectra (Pb 4f and N1s) of the $MAPbBr_3$ films and $MAPbBr_3$@PAN composite films.

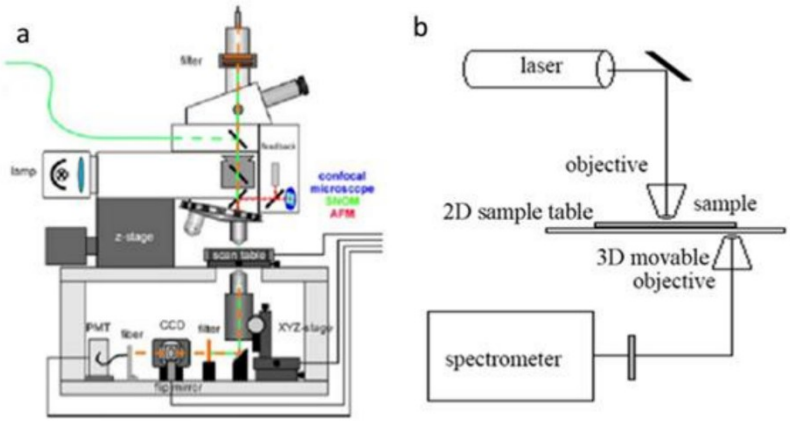

Fig. S4 Schematic illustration of the home-built micro-photoluminescence (μ-PL) setup used for lasing measurements.

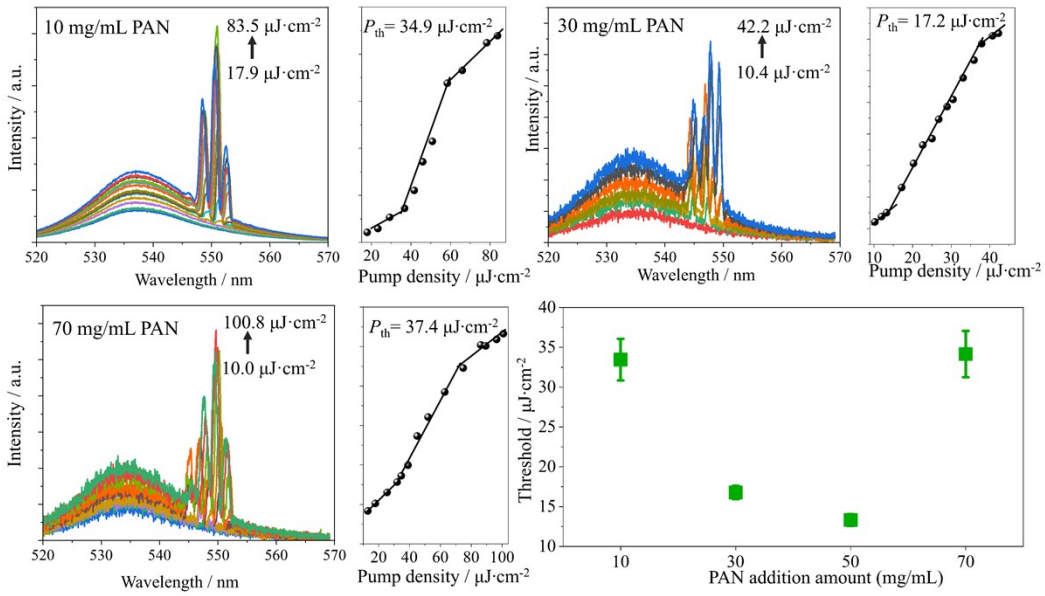

Fig. S5 Pump-fluence-dependent PL characterization of $MAPbBr_3$@PAN composite films with different PAN addition amounts.

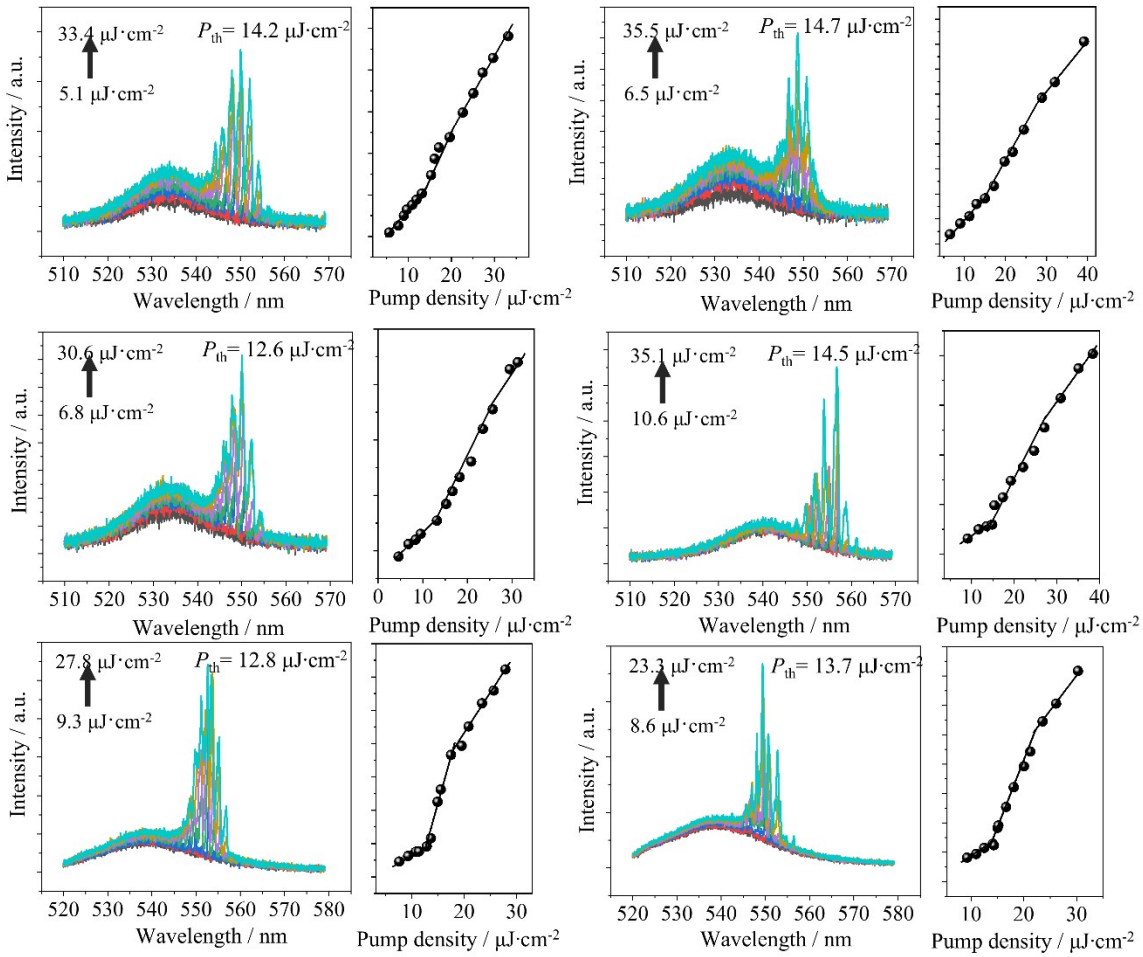

Fig. S6 Pump-fluence-dependent PL characterization of $MAPbBr_3$@PAN micro-rings for lasing threshold statistics in Figure 2c.

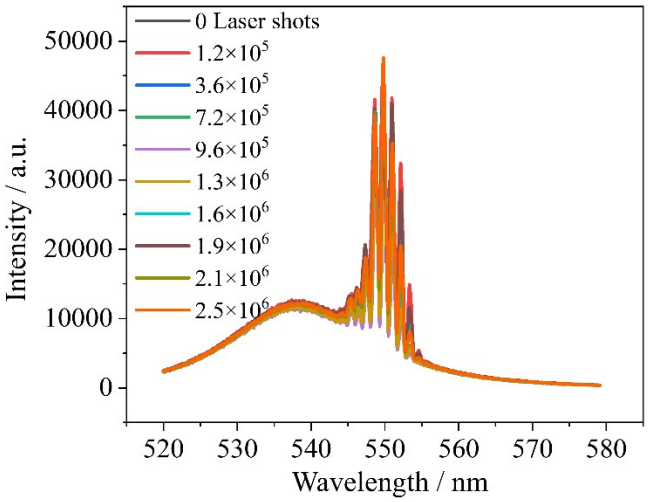

Fig. S7 Laser spectral stability of $MAPbBr_3$@PAN micro-ring under high humidity conditions (20 ℃, 60% humidity).

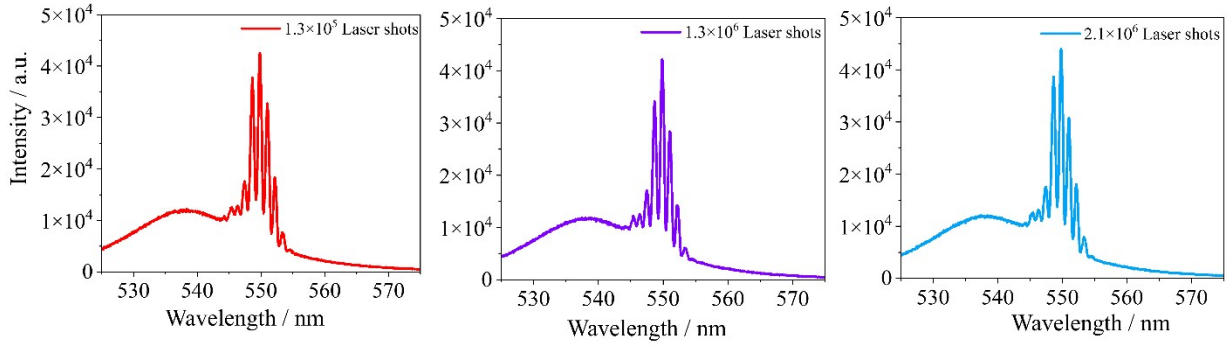

Fig. S8 The lasing spectra of $MAPbBr_3$@PAN micro-ring uder different laser shots.

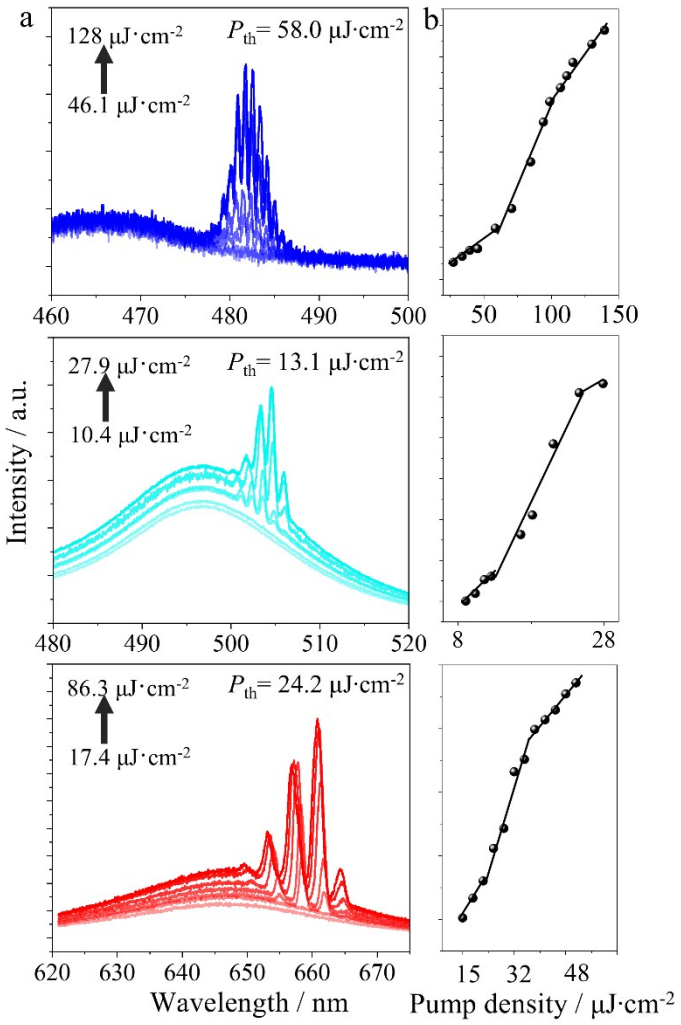

Fig. S9 (a) μ-PL spectra of $MAPbX_3$@PAN micro-rings (b) Integrated μ-PL intensities versus pump density.

Tab. S1 Comparative summary of key parameters in micro/nanolaser arrays.

Materials	Lasing mode	Pump source	Threshold ($\mu J \cdot cm^{-2}$)	Lasing wavelength(nm)	Q	Year	Ref
$MAPbI_3$	WGM	400nm,50fs, 1kHz	~15	~792	1210	2016	[1]
$MAPbBr_3$	FP	400nm,100fs, 1kHz	5.9	~542		2016	[2]
$MAPbBr_3$	WGM	400nm,150fs, 1kHz	15.9	549		2016	[3]
$MAPbBr_3$	WGM	400nm,150fs, 1kHz	3.5	553	1090	2016	[4]
$CsPbCl_3$	WGM	400nm, 120fs, 1kHz	15	426	1032	2017	[5]
$MAPbBr_3$	WGM	400nm,100fs, 1kHz	4.9	546	~800	2017	[6]
$MAPbBr_3$	FP	400nm,150fs, 1kHz	12.3	543	500	2017	[7]
$MAPbBr_3$	WGM	400nm,100fs, 1kHz	3.5	545	3000	2017	[8]
$BA_2FA_5Pb_6Br_{19}$	WGM	400nm, 150fs, 1kHz	27.2	546-553	1800	2018	[9]
$BA_2MA_5Pb_6Br_{19}$	WGM	400nm, 150fs, 1kHz	12.2	~543	2600	2018	[10]
$OA_2MA_{n-1}Pb_nBr_{3n+1}$	WGM	400nm, 150fs, 1kHz	~8	~545		2018	[11]
$MAPbI_3$	WGM	400nm, 100fs, 1kHz	59.2	~780		2018	[12]
$CsPbBr_3$	WGM	400nm,60fs	~3	~550	1555	2019	[13]
$CsPbBr_3$			3	530		2019	[14]
$CsPbBr_3$ QDs	FP	400nm, 120fs, 1kHz	37.6	~536		2020	[15]
$MAPbBr_3$		400nm	70.8	~530	885	2020	[16]
$MAPbBr_3$	WGM	400nm, 100fs, 1kHz	16.2	~551		2020	[17]
$CsPbBr_3$	WGM	400nm, 200fs, 1kHz	4	545	6806	2020	[18]
$CsPbBr_3$ NCs	WGM	400nm, 250fs	3.8	~530	2200	2021	[19]
$CsPbBr_3$	Random laser	400nm, 100fs, 1kHz	25	~540		2021	[20]
$MAPbBr_3$	FP	400nm, 100fs, 1kHz	43.7	549	1483	2021	[21]
$FAPbBr_3$	FP	400nm, 100fs, 1kHz	19.9	~550	2404	2021	[21]
$CsPbI_3$	WGM	800nm, 30fs, 1kHz	0.22	649		2021	[22]
$CsPbBr_3$		400nm, 120fs, 1kHz	18.8	~540	~1000	2022	[23]
$MAPbBr_3$	WGM	400nm, 150fs, 1kHz	15.1	~550	~1000	2022	[24]
$MAPbBr_3$	WGM	400nm, 50fs, 1kHz	35	~550	1135	2023	[25]
$CsPbBr_3$		400nm, 150fs, 1kHz	40	540		2023	[26]
$MAPbBr_3$	WGM	395nm, 1kHz	4.14	555	2915	2023	[27]
$CsPbBr_3$	Random laser	400nm, 100fs, 1kHz	8.3	539	1740	2024	[28]
$MAPbBr_3$	WGM	450nm, 50ns,10Hz	14	556	1544	2024	[26]
$BA_2Cs_{n-1}Pb_nBr_{3n+1}$	FP	400nm, 50fs, 1kHz	7.8	560	2340	2024	[29]
$MAPbBr_3$	WGM		14.7	549	2113	2025	[30]
$CsPbBr_3$ QDs	WGM	400nm, 150fs, 1kHz	6.6	530	1808	2025	[31]
$CsPbBr_3$ QDs		400nm, 50fs, 1 kHz	15	540		2026	[32]
$MAPbBr_3$@PAN	WGM	400nm, 1 kHz	12.8	545	2126	This work	

[1] X. Liu, L. Niu, C. Wu, C. Cong, H. Wang, Q. Zeng, H. He, Q. Fu, W. Fu, T. Yu, C. Jin, Z. Liu and T. Sum, *Adv. Sci.*, 2016, **3**, 1600137.

[2] K. Wang, Z. Gu, S. Liu, W. Sun, N. Zhang, S. Xiao and Q. Song, *J. Phys. Chem. Lett.*, 2016, **7**, 2549 – 2555.

[3] Z. Gu, K. Wang, H. Li, M. Gao, L. Li, M. Kuang, Y. Zhao, M. Li and Y. Song, *Small*, 2017, **13**, 1603217.

[4] J. Feng, X. Yan, Y. Zhang, X. Wang, Y. Wu, B. Su, H. Fu and L. Jiang, *Adv. Mater.*, 2016, **28**, 3732 – 3741.

[5] X. He, P. Liu, H. Zhang, Q. Liao, J. Yao and H. Fu, *Adv. Mater.*, 2017, **29**, 1604510.

[6] K. Wang, W. Sun, S. Wang, S. Liu, N. Zhang, S. Xiao and Q. Song, *Adv. Optical Mater.*, 2017, **5**, 1600744.

[7] P. Liu, X. He, J. Ren, Q. Liao, J. Yao and H. Fu, *ACS Nano*, 2017, **11**, 5766 – 5773.

[8] Z. Duan, Y. Wang, G. Li, S. Wang, N. Yi, S. Liu, S. Xiao and Q. Song, *Laser & Photonics Rev.*, 2018, **12**, 1700234.

[9] H. Zhang, Y. Wu, Q. Liao, Z. Zhang, Y. Liu, Q. Gao, P. Liu, M. Li, J. Yao and H. Fu, *Angew. Chem. Int. Ed.*, 2018, **57**, 7748 – 7752.

[10] H. Zhang, Q. Liao, Y. Wu, Z. Zhang, Q. Gao, P. Liu, M. Li, J. Yao and H. Fu, *Adv. Mater.*, 2018, **30**, 1706186.

[11] M. Li, Q. Wei, S. Muduli, N. Yantara, Q. Xu, N. Mathews, S. Mhaisalkar, G. Xing and T. Sum, *Adv. Mater.*, 2018, **30**, 1707235.

[12] C. Huang, W. Sun, Y. Fan, Y. Wang, Y. Gao, N. Zhang, K. Wang, S. Liu, S. Wang, S. Xiao and Q. Song, *ACS Nano*, 2018, **12**, 3865 – 3874.

[13] Z. Yang, J. Lu, M. ZhuGe, Y. Cheng, J. Hu, F. Li, S. Qiao, Y. Zhang, G. Hu, Q. Yang, D. Peng, K. Liu and C. Pan, *Adv. Mater.*, 2019, **31**, 1900647.

[14] A. Schlaus, M. Spencer, K. Miyata, F. Liu, X. Wang, I. Datta, M. Lipson, A. Pan and X. Zhu, *Nat. Commun.*, 2019, **10**, 265.

[15] X. Hu, C. Lu, Q. Wang, J. Xu and Y. Cui, *Rsc Adv.*, 2020, **10**, 38220 – 38226.

[16] S. Li, H. Xia, G. Zhang, X. Xu, Y. Yang, G. Wang and H. Sun, *Adv. Mater. Technol.*, 2020, **5**, 2000051.

[17] K. Wang, Y. Du, J. Liang, J. Zhao, F. Xu, X. Liu, C. Zhang, Y. Yan and Y. Zhao, *Adv. Mater.*, 2020, **32**, 2001999.

[18] Z. Gu, Z. Zhou, Z. Huang, K. Wang, Z. Cai, X. Hu, L. Li, M. Li, Y. Zhao and Y. Song, *Adv. Mater.*, 2020, **32**, 1908006.

[19] D. Xing, C. Lin, Y. Ho, A. Kamal, I. Wang, C. Chen, C. Wen, C. Chen and J. Delaunay, *Adv. Funct. Mater.*, 2021, **31**, 2006283.

[20] X. Chen, K. Wang, B. Shi, T. Liu, R. Chen, M. Zhang, W. Wen, G. Xing and J. Wu, *ACS Appl. Mater. Interfaces*, 2021, **13**, 30891 – 30901.

[21] S. Yan, K. Wang, G. Xing, J. Xu, S. Su, Z. Tang, S. Wang and K. Ng, *ACS Appl. Mater. Interfaces*, 2021, **13**, 38458 – 38466.

[22] S. Lan, Y. Peng, H. Shen, S. Wang, J. Ren, Z. Zheng, W. Liu and D. Li, *Laser & Photonics Rev.*, 2021, **15**, 2000428.

[23] J. Liang, K. Wang, Y. Du, C. Zhang, Y. Yan and Y. Zhao, *ACS Appl. Mater. Interfaces*, 2022, **14**, 1774 – 1782.

[24] Z. Zhang, F. Vogelbacher, J. De, Y. Wang, Q. Liao, Y. Tian, Y. Song and M. Li, *Angew. Chem. Int. Ed.*, 2022, **61**, e202205636.

[25] P. Ma, L. Yan, J. Si, T. Huo, Z. Huang, W. Tan, J. Xu and X. Hou, *Laser & Photonics Rev.*, 2023, **17**, 2300533.

[26] A. Berestennikov, S. Kiriushechkina, A. Vakulenko, A. Pushkarev, A. Khanikaev and S. Makarov, *ACS Nano*, 2023, **17**, 4445 – 4452.

[27] Z. Xu, X. Han, W. Wu, F. Li, R. Wang, H. Lu, Q. Lu, B. Ge, N. Cheng, X. Li, G. Yao, H. Hong, K. Liu and C. Pan, *Light-Science & Applications*, 2023, **12**, 67.

[28] Y. Tan, L. Yang, H. Song, M. Huang, J. Huang, W. Ali, F. Li and Z. Li, *Small*, 2024, **20**, 2401596.

[29] C. Zhao, J. Guo, J. Tao, J. Chu, S. Chen and G. Xing, *Light-Science & Applications*, 2024, **13**, 170.

[30] B. Liu, J. Guo, H. Zhang, Y. Tang, L. Qin, Z. Lou, Y. Hu, F. Teng and Y. Hou, *J. Mater. Chem. C*, 2025, **13**, 6233 – 6239.

[31] Y. Ding, H. Zhang and H. Fu, *J. Phys. Chem. Lett*, 2025, **16**, 6781 – 6786.

[32] S. Zheng, Q. Ji, Y. Chen, W. Shao, C. Guo, B. Zhu, Y. Chen, J. Yu and S. Deng, *ACS Nano*, 2026, **20**, 7228 – 7237.